ELSEVIER

Coastal Engineering 37 (1999) 471–485

COASTAL ENGINEERING

www.elsevier.com/locate/coastaleng

Some observations of wave–current interaction

J. Wolf *, D. Prandle

CCMS, Proudman Oceanographic Laboratory, Bidston Observatory, Birkenhead, Merseyside, L43 7RA, UK

Abstract

Using data collected during the SCAWVEX Project, the effect of depth and current changes (particularly tidal) on waves and the effect of waves on tidal currents were examined. The possible interaction mechanisms between waves, tides and surges are reviewed. These include the effective surface wind stress, bottom friction, depth and current refraction and modulation of the absolute and relative wave period. The usefulness of tidal periodicity in identifying both interactions in wave parameters and the effects of the waves on the tide is noted. For correct analysis, to obtain wave-free tidal conditions or tidally-averaged wave statistics, it is particularly important to understand the interaction mechanisms. For example, the amplitude of the tidal current was found to be reduced in periods of high waves. Ideally, waves and currents should always be measured simultaneously since the correct determination of either in shallow water requires knowledge of the other. Various remote sensing systems which can potentially do this are discussed. Since the algorithms are quite complex and may depend on a good 'first guess', the future probably lies in combining remote sensing plus modelling together with ground truth 'in situ' data.

Keywords: Wave–current interaction; Tidal currents; Bottom friction

1. Introduction

Applications of wave and current data both coastal and offshore include the oil and gas industry (rigs, pipelines, ship operations), ship routing, coastal protection, waste disposal (planned and accidental), ecological (oxygen, temperature distribution and stratification, sedimentological studies, wave and tidal energy devices and flood warning. Eventually, data collected continuously (in real time) may be available for monitoring, determination of long-term statistics and assimilation into operational models.

* Corresponding author. Fax: +44-151-653-6269; E-mail: judith_wolf@compuserve.com

PII: S0378-3839(99)00039-3

Wave–current interactions can occur over a wide range of both wave and current conditions; here we restrict consideration to surface waves (0.1 to 0.5 Hz) and barotropic tidal currents. The important effect of surface waves on the generation of wind-driven surge currents is omitted, as is wave-generated mean flow. Two aspects are highlighted: (i) the effect of waves on enhancing the bottom friction experienced by tidal currents, and (ii) the effect of tidal currents on the propagation of surface waves. The latter problem includes consideration of techniques for 'correcting' observed wave spectra to remove current modulation. Since wave–current interaction will be shown, in certain circumstances, to be of major importance, one objective of this study is to define these circumstances where both parameters need to be measured simultaneously and methods of doing this are discussed.

A review of wave–current interaction is given by Jonsson (1990). Wave kinematics (changes in the wavenumber and frequency due to shoaling and refraction, in the absence of sources and sinks of energy) and dynamics (changes in wave height, wave action conservation, effects of wind input and dissipation) can often be dealt with independently (strictly only if wave motion does not influence the current field, e.g., through radiation stress or increased bed shear). Wave kinematics include the effect of depths and currents in the dispersion relation (Doppler shift) and changes in wavelength due to an opposing or following current. There are different effects for homogeneous or inhomogeneous currents and steady or unsteady flow. Wave dynamics include set-down, energy and action conservation, producing changes in wave height or mean level. Jonsson also discusses the effects of depth-varying currents, however, these will not be considered here, being more important in wind-driven surge flows than in tidal currents. Methods of deriving an equivalent uniform current can be used, e.g., Hedges and Lee (1992). Soulsby et al. (1993) discuss wave–current interaction in the vertical dimension, including bottom friction and wave kinematics but also wave-induced mass transport. They show that good predictions of wavelength and bottom orbital velocity can be obtained using a mean current approximation. Tolman (1990, 1991a,b) demonstrates the effect of currents in wave models on the NW European continental shelf, showing that the currents must be treated as unsteady. Burrows and Hedges (1985) show the effects of currents on integrated wave parameters. Hedges (1987) states that it is important to include interaction in the following situations: the analysis of bottom pressure records for waves (e.g., Wolf, 1997), and calculations of energy spectra, refraction, forces on structures and extreme waves.

During the EC MAST SCAWVEX Project (Surface Current and Wave Variability Experiment), several datasets were collected in the near-shore region of the North Sea. A large part of the project was concerned with the development and evaluation of HF radar but here we refer mainly to the results of in situ measurements. Several stations were located off the Holderness coast (NE England) during the winters of 1994/1995 and 1995/1996 (N1 in 12.5 m water depth and N2 in 18 m). The other stations were off the Rhine (Maasmond) in February–April 1996 (in 18 m depth) and Petten in November–December 1996 (in 22 m depth). Both the latter are near the coast of the Netherlands. The stations are all situated in open coastal conditions, although the Maasmond station is more sheltered from wave energy. These datasets include measurements made by the commonly-used Datawell Directional Waverider (DWR) buoys, bottom pressure measurements and, particularly valuable, near-bed recordings by the InterOcean S4DW which incorporates an electro-magnetic current meter, giving high frequency currents and hence an estimate of the directional wave spectrum.

In this paper, we first attempt to give a comprehensive review of the potential interaction mechanisms between waves and currents, then illustrate some of these by reference to observations. Implications for wave modelling and monitoring are discussed.

2. Theoretical background

The main energy in the coastal region is due to tides, surges, and wind waves. Interactions occur between these different 'waves' because the tides and surges change the mean water depth and current field experienced by the waves. Surges and tides are both long waves with periods of several hours. Surface gravity waves (wind waves) have periods of several seconds. Thus, the surge and tidal currents appear to the wind waves as quasi-steady over measurement periods of 10–20 min. Interactions between surge and tide are discussed elsewhere, e.g., Prandle and Wolf (1978). The effects of currents (mainly tidal) on waves and waves on currents are discussed below.

Linear wave theory should be sufficiently accurate in the depths of water concerned for Holderness, Maasmond and Petten (i.e., greater than 12.5 m mean depth), with significant wave heights less than 5 m, for the purposes of dispersion.

2.1. Effects of currents on waves

Various mechanisms for interaction are summarised as follows, the effects of wind and current shear are referred to for completeness although not discussed further here.

(i) Wave generation by wind—the effective wind is that relative to the surface current, and the wave age (c_p/U^*) and effective surface roughness may be important, e.g., Janssen (1989). Here c_p is the wave phase speed and U^* is the friction velocity of the wind. The effective fetch also changes in the presence of a current.

(ii) Wave propagation—the effects of depth refraction are easy to spot, turning the mean wave direction towards shore-normal. Current refraction has a more subtle effect, dependent on the spatial variation of currents, whether decreasing or increasing towards the coast. Generally shoaling depths will increase the tidal amplitude towards the coast until friction reverses this trend. The waves will tend to turn towards the direction of the current axis.

(iii) Doppler shift—the effect of a steady current on intrinsic (relative) wave frequency. Waves of the same apparent (absolute) period will have a longer intrinsic period in a favourable (following) current and a shorter intrinsic period in an opposing current.

(iv) Steepening of waves on an opposing current (related to (iii)), due to shorter wavelength and increased wave height from wave action conservation.

(v) Modulation of absolute frequency by unsteady currents and modulation of intrinsic frequency by propagation over spatial gradients of current. If the current is steady the absolute frequency should be constant, if the current is homogeneous the intrinsic frequency should be constant. If both intrinsic and absolute period show a tidal modulation, the currents must be effectively inhomogeneous and unsteady.

(vi) Wave–current bottom stress. Various empirical theories for wave–current interaction in the bottom boundary layer suggest that the friction coefficient experienced by waves in a current regime will be larger than in no current. This also applies to the effective current friction factor in the presence of waves.

(vii) Effect of vertical current shear on wave breaking. Wind-driven surge currents would be relevant to this, the tidal currents considered here have no surface shear.

The wave intrinsic (angular) frequency, σ, is related to the wave number, k, by the dispersion relation:

$$\sigma = \sqrt{gk \tanh kh}\,, \tag{1}$$

in water depth h, whereas the observed or apparent (absolute) frequency, ω, is Doppler-shifted:

$$\omega = \sigma + \boldsymbol{k} \cdot \boldsymbol{U}, \tag{2}$$

where $\boldsymbol{k}$ is the wave-number vector and $\boldsymbol{U}$ the current vector, e.g., Phillips (1977).

The time variation of absolute frequency is given by:

$$\frac{\mathrm{d}\omega}{\mathrm{d}t} = \frac{\sigma k}{\sinh 2kh}\frac{\partial h}{\partial t} + \boldsymbol{k} \cdot \frac{\partial \boldsymbol{U}}{\partial t} = k\left\{C\frac{\partial h}{\partial t} + \frac{\partial U_{\mathrm{c}}}{\partial t}\right\}, \quad \text{where } C = \frac{\sqrt{gk \tanh kh}}{\sinh 2kh}\,,$$
$$U_{\mathrm{c}} = U\cos(\delta - \alpha) \tag{3}$$

(Jonsson, 1990). Here, t is time, δ is the current direction, and α the wave direction. This shows that the variation with time is related to the time variation of depth and relative current. In 'deep' water $(h > L/2$, wavelength $L = 2\pi/k)$ the depth-related component disappears. The time derivative of the intrinsic frequency is

$$\frac{\mathrm{d}\sigma}{\mathrm{d}t} = -\frac{\sigma kh}{\sinh 2kh}\nabla \cdot \boldsymbol{U} - c_{\mathrm{g}}\boldsymbol{k} \cdot \frac{\partial \boldsymbol{U}}{\partial s} \tag{4}$$

where c_{g} is the wave group speed and $\partial/\partial s$ the space derivative in the direction of wave propagation.

In order to look for the classical steepening effect of waves on an opposing current we need to use the intrinsic or relative frequency (which is directly related to wavelength). The significant steepness parameter

$$S_{\mathrm{S}} = \frac{2\pi H_{\mathrm{S}}}{gT_{\mathrm{Z}}^2} \tag{5}$$

gives a good approximation to the steepness $H_{\mathrm{S}}/L_{\mathrm{M}}$ (where L_{M} is the mean wavelength $= 2\pi/\int kE(f)\mathrm{d}f$) if the relative (intrinsic) T_{Z} is used.

Current refraction is governed by Snell's law: $k \sin \beta =$ constant, where β is the angle between wave direction and the normal to current direction, i.e.,

$$\frac{\sin\beta_2}{\sin\beta_1} = \frac{L_2}{L_1} \tag{6}$$

(Jonsson, 1990). In this case, the values β_1 and L_1 represent the incident angle and wavelength in one current regime (U_1), β_2 and L_2 represent the angle with the normal and wavelength in a second current regime (U_2). T_a is the apparent wave period.

2.2. Effects of waves on currents

(i) Radiation stress—leading to longshore currents (and set-up). This effect will be most noticeable very near shore and is not discussed further.

(ii) The effective surface drag coefficient for wind-driven surge currents may change with wave age. This was discussed in (Wolf et al., 1988) and developed by Janssen (1989) but will not be considered further. It is still difficult to demonstrate that this effect is important in practice. Work is proceeding on analysis of surface stress measurements from South Wales and off Nova Scotia (Peter Taylor, personal communication).

(iii) The bottom friction coefficient for currents will be modified in the presence of waves. We will concentrate on the effect of bottom friction on tidal currents.

Prandle (1997a) shows that bottom friction has little effect on depth-averaged tidal current in water depths greater than 50 m. This demarcation is dependent on: (a) the period of the tidal constituent (diurnal more sensitive than semi-diurnal), (b) the latitude (most sensitive to friction at the respective inertial latitudes), and (c) the magnitude of the tidal current. However, in deeper water, the magnitude of the bottom friction does influence the near-bed vertical profile of current. Prandle (1982) illustrates quantitatively how the respective vertical profiles for clockwise and anti-clockwise rotating tidal components are influenced by both bottom friction and vertical eddy viscosity.

3. Observations

Various media are used to measure waves and currents including mechanical, acoustic, electromagnetic, radar and optical devices; in situ (e.g., the Datawell Directional Waverider surface-following buoy) or by remote sensing such as HF radar. Some can measure waves and currents simultaneously (e.g., radar) and, while this may be an advantage in a coastal monitoring system, careful checks need to be made on the assumptions which are used in obtaining the waves and currents due to the interaction processes already mentioned.

The results discussed here are derived from analysis of the in situ wave and current data collected during the SCAWVEX Project. These include measurements made by the commonly-used Datawell Directional Waverider buoys and bottom pressure measurements, particularly those made by the InterOcean S4DW which incorporates an electromagnetic current meter, giving near-bed high frequency currents and hence an estimate of the directional wave spectrum. The availability of the current measurements allows a more accurate estimate of the wavenumber from the Doppler equation and therefore a more accurate correction for depth-attenuation of the bottom pressure. This can be significant for waves measured in moderate tidal currents (up to ~ 0.7 m/s), e.g., Wolf (1997).

4. Effects of currents on waves

4.1. Effects on wave height, period and steepness

The tidal-period modulation of H_S and T_Z which is observed by the Waverider (see Fig. 1) can come from two sources: the relative motion of the mooring about its central position and the effects of the unsteady depth and current on the absolute frequency. The former could mean that the buoy is particularly bad at responding correctly to the wave motion at times of maximum current. This would be likely to reduce the observed wave height at these times, but the observed period would probably be unaffected. The unsteady current and depth affect mainly the period. The observed modulations are mainly in period, suggesting the latter effect is predominant. Note that at Holderness, stations N1 and N2, the depth and current variation are almost 90° out of phase, whereas at Maasmond and Petten, the current leads the depth variation by only 30°. The time variation of the intrinsic wave period is related to the spatial gradients of current.

The bottom currents observed by the S4DW, corrected to approximate surface values by a constant amplification factor, were used to compute the intrinsic period for the DWR data. Despite the small change in actual values of the wave period, this had a noticeable effect, especially on the time sequence of the intrinsic wave steepness calculated as in Eq. (5). The maximum steepness was delayed by up to 2 h relative to the steepness calculated using the absolute wave period. Fig. 2 shows an extract from the time series of steepness and relative current for December 1994. The intrinsic steepness can be seen to lag the absolute steepness. The maximum correlation of steepness with relative current for the whole Holderness experiment is with a time lag of 3 h, not 6 h as would be expected if the maximum steepness corresponded to the maximum opposing current. Using T_Z (absolute) the maximum steepness occurs just after the maximum following current. Based on Doppler shift alone, the expected behaviour would be maximum absolute steepness with a following current and minimum with an opposing current. These results indicate that spatial gradients of current, as well as unsteady depth and current, are important in this area. If the waves travelled through the area of non-uniform tidal current faster than the time-scale of change of the current the expected maximum intrinsic steepness would be at the time of maximum opposing current, however this is obviously not the case. Note that part of the modulation in

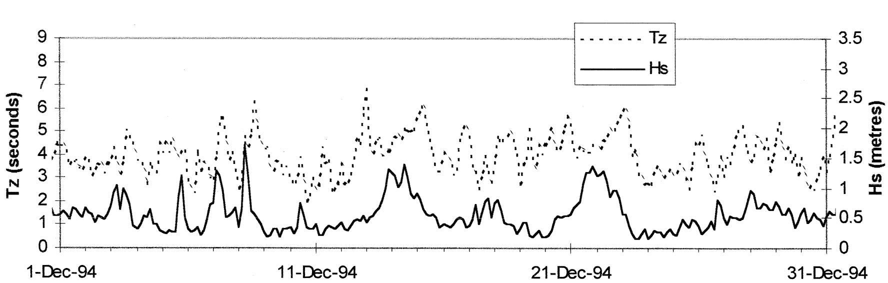

Fig. 1. Time series of H_S, T_Z for December 1994 at N1.

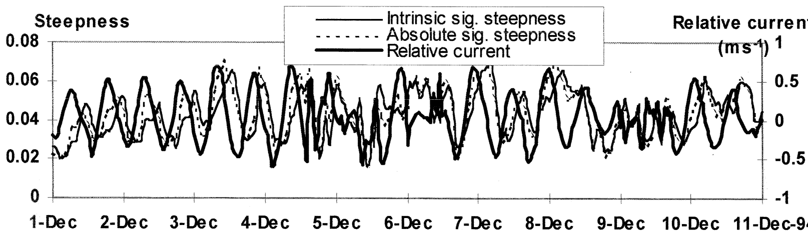

Fig. 2. Wave steepness and relative current (in the direction of wave propagation) at N2.

steepness is due to modulation of the wave height by time-varying depth but this appears to be a small contribution.

4.2. Effects on wave direction

Another manifestation of wave–current interaction is in the tidal modulation of the high frequency wave direction. Some examples, selected at times when this modulation is most apparent, are seen in Fig. 3, where the wave direction (from which the waves are approaching) at 0.5 Hz is plotted for the DWR at N2. Also plotted are the current direction from the S4DW data and the wind direction (from the coastal station at Donna Nook), which would be expected to be approximately coincident with the wave direction for high frequency waves.

Examination of the mean wave direction shows a marked tidal modulation, especially at about 0.5 Hz or above. The examples shown demonstrate that current refraction is the likely mechanism for different situations of wave incident direction relative to the tidal

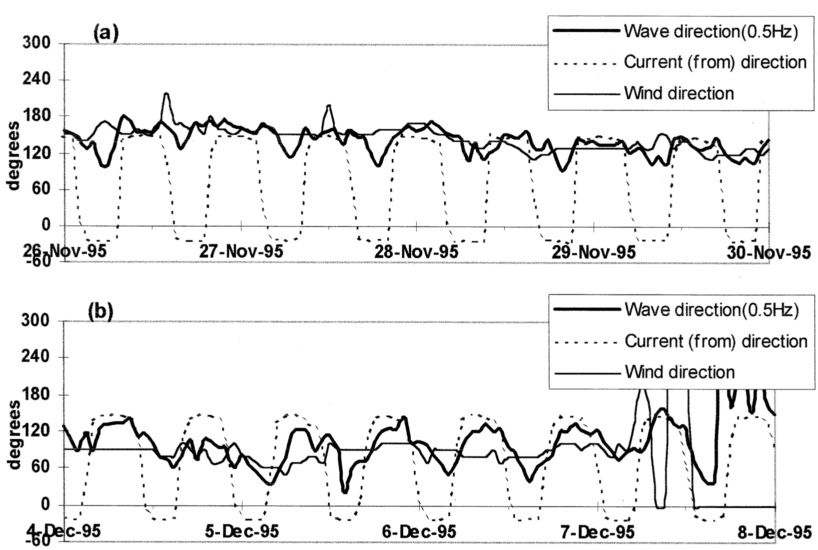

Fig. 3. Tidal modulation of high frequency wave direction at N2.

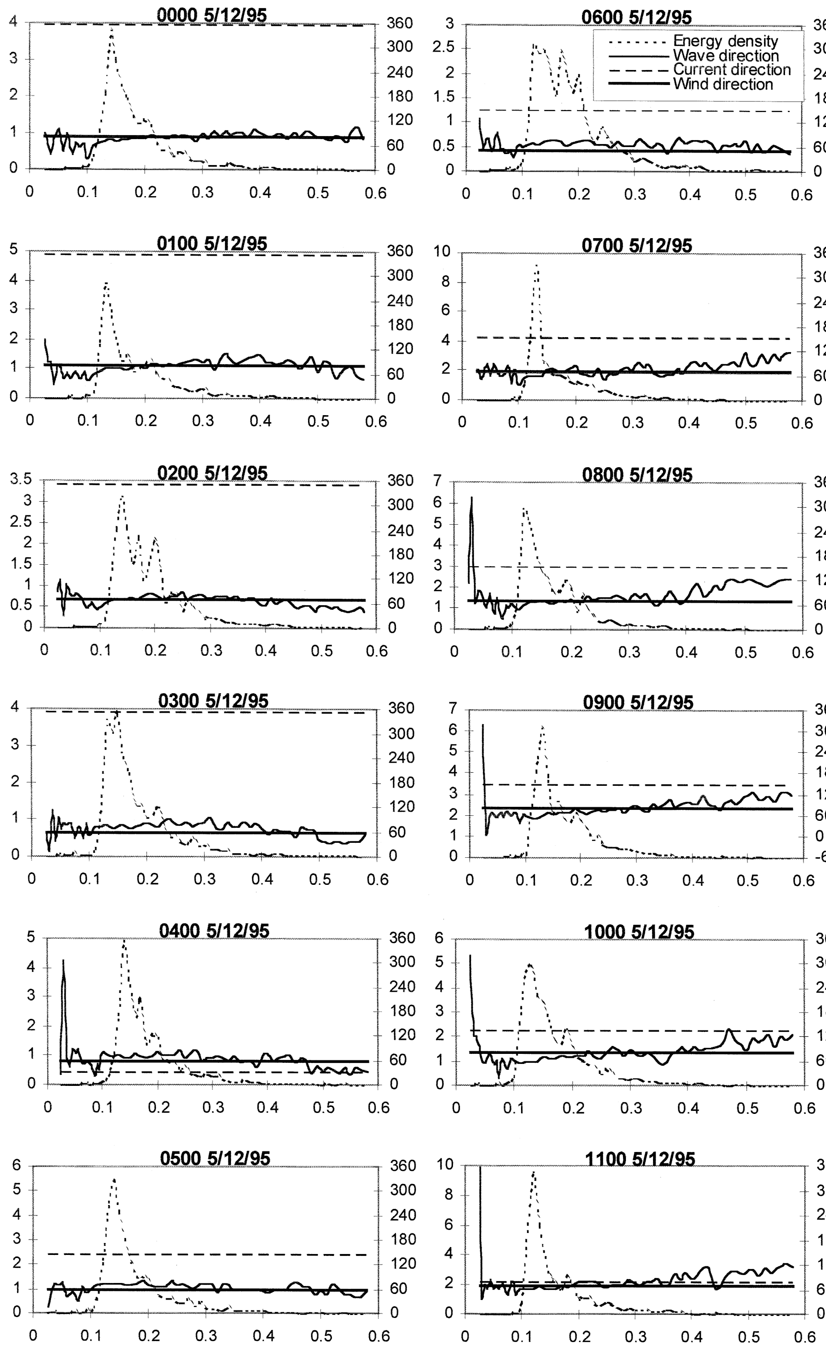

Fig. 4. Wave spectra for 5 December 1995. The higher frequency waves can be seen to be turning increasingly towards the current direction as the frequency increases.

current. The maximum turning effect will occur for the shortest waves when the waves are incident at about 45° to the current. The predominant current direction is 330°/150° so waves from 285°, 015°, 105° or 195° are likely to show the maximum modulation in direction. Note that the current direction is shown as a 'from' direction, opposite to the normal convention, for ease of comparison with the standard wind and wave 'from' direction. Fig. 3(a) is for 26–30 November 1995, when the wind is persistently from SE (150°), i.e., parallel to the shore and producing waves almost collinear with the tidal current. No turning occurs for waves with a following current, but when the current is opposing the waves they start to turn towards the current direction. Fig. 3(b) is for 4–8 December 1995, when the wind is from the east (090°), close to the optimum direction of 45° to the current for maximum refraction. The high frequency wave direction can be seen to deviate from the wind direction in such a way as to bring it towards the current direction. There is a limit in absolute (apparent) frequency at $-g/4U$ for collinear waves and currents when there can be no wave propagation against the counter-current. An opposing current of 0.78 m/s is required for the 0.5 Hz waves. Effects on wave spectra are seen in Fig. 4 for the second case, described for Fig. 3(b). The higher frequency waves can be seen to be turning increasingly towards the current direction as the frequency increases. This would appear consistent with current refraction derived from Eq. (6), although detailed knowledge of the spatial current gradients is not available.

5. Effects of waves on currents

In order to investigate the effects of waves on currents we focus on the tidal component of current which can be more easily separated due to its known periodicity. The time series of mean currents was subjected to a Fourier analysis for the amplitude

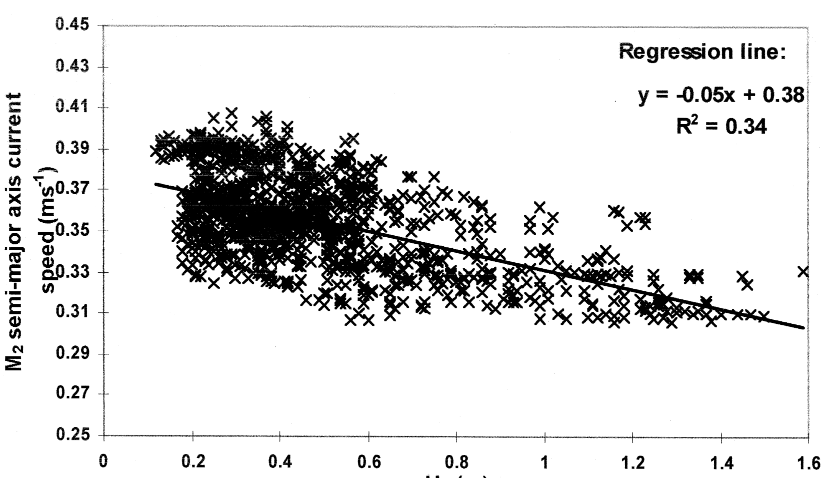

Fig. 5. Amplitude of semi-diurnal tidal current vs. wave height at N1.

and phase of the dominant M_2 constituent (period 12.42 h) using successive overlapping 25-h time segments. This produced an hourly time series of the amplitude and phase of the east and north component of the main semi-diurnal component of the tidal current, which were combined to give ellipse parameters, in particular the semi-major axis amplitude. Since it is not possible to separate the M_2 and S_2 constituents within 25 h, this time series is modulated in particular by the spring-neap variation. A large amount of the variance was removed by Fourier analysis for the fortnightly and monthly (MS_f and M_m) constituents. The remainder is a measure of the amplitude of the mean semi-diurnal current component. This has been plotted against wave height in Fig. 5. The amplitude of the tidal current may be seen to tend to decrease with increasing wave height (that this is not the reverse effect of wave height decreasing with increased tidal current can be seen by inspection of the relevant time series plots, not shown here). This effect is quantified further below.

Fig. 6 shows, for position N1, how the tidal current amplitude is reduced as a function of both the magnitude and direction of the waves relative to the current. In this

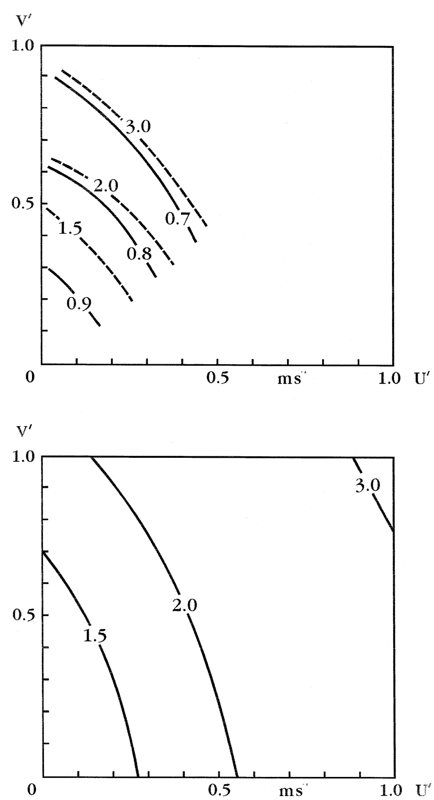

Fig. 6. Top: continuous line shows observed R'/R (where $R=$ tidal current, $R'=$ tidal current amplitude reduced by waves, $U'=$ wave current orthogonal to R, $V'=$ wave current parallel to R), dashed line shows k'/k ($k'=$ wave enhanced bed friction coefficient). Bottom: k'/k from Grant and Madsen (1979). Data from N1.

diagram the amplitude of the tidal current is normalised by reference to the tidal elevation amplitude, i.e., a linear relationship is assumed between the tidal current amplitude and the tidal elevation amplitude for successive intervals of 12.5 h. This device removes the spring-neap effect on variability in tidal currents.

The reference value of unity corresponds to the maximum tidal currents observed in the absence of waves. The wave influence is characterised by the sea bed orbital velocity and direction corresponding to H_S and T_P. The observed tidal current amplitude is shown to reduce to less than 70% of its undisturbed value for (orthogonal) wave orbital velocities of 1.0 ms^{-1}.

6. Implications for modelling of combined waves and currents

6.1. Effect of bottom friction on tidal current amplitude

Fig. 6 shows the variation in tidal current amplitude (for conditions specific to Holderness station N1) as a function of the wave current parallel and orthogonal to the tidal current. Translating these results into the observed decrease in tidal current amplitude in the presence of waves, enables the associated contours to be converted to related bed stress coefficients. A second set of contours shown in Fig. 6 indicates the calculated bed stress coefficients, k'/k, for this tide-current regime obtained from the theory of Grant and Madsen (1979) (k' is the friction coefficient in the presence of waves while k is the undisturbed value). While there is qualitative agreement, there is significant quantitative discrepancy. Soulsby et al. (1993) reviews a series of such wave-current bed friction algorithms and illustrates similar divergence. It seems likely that the precise nature of wave–current interactive effects on bottom friction will be sensitive to the nature of the localised sea bed conditions. Wolf (1998) (this volume) supports this and shows that the model of Christoffersen and Jonsson (1985) is in reasonable agreement with the S4DW data. In the absence of a universally applicable formulation, the present exercise emphasises the importance of localised observations to provide suitable algorithms for wider scale tidal, wave and sediment transport simulations.

6.2. Effect of tidal currents on wave propagation

Wolf (1998) (this volume) looks at the variation of the wave friction coefficient with current. The near-bottom currents measured by the S4DW wave–current meter have been separated into mean, wave and turbulent components. The latter are assumed to be related to the bottom friction shear stress and used to calculate an effective wave and current friction coefficients, f'_W and f'_C (f'_C corresponds to k' referred to in Fig. 6).

The following results were noted.

(a) f'_C increases with increasing U_W.

(b) f'_W decreases with increasing U_W and increases with increasing U_C, where U_W and U_C are the magnitude of the wave and current velocities, respectively.

Note that results (a) and (b) are consistent with the theory of Grant and Madsen (1979) and Christoffersen and Jonsson (1985).

6.3. The WAM wave model

The general release (cycle 4) of the 3rd-generation wave model WAM (Komen et al., 1994) now includes depth and current refraction (Hubbert and Wolf, 1991) although so far for a steady current field. In Section 3, it has been shown that the assumption of a steady current may not be adequate. The bottom friction used in the model does not allow for interaction with currents, being based on the JONSWAP results (Hasselmann et al., 1973) with a constant friction coefficient. For further development of numerical models, the detailed physical processes need to be understood. For example, the WAM model is being applied in the Holderness region (Wolf and Hargreaves, 1998). One question to be answered is whether sufficient detail can be resolved to distinguish between, for example, different parameterisations of the wave–current bottom stress. Various models have been presented, e.g., Grant and Madsen (1979), Christoffersen and Jonsson (1985), Madsen (1995) which have been incorporated into the modified version of WAM (here referred to as POLWAM, Luo et al., 1997). Tolman (1992) has questioned the value of these more complex formulations, because the experimental datasets which he has re-analysed seem to show the friction coefficients varying in the opposite direction to the models. Ultimately these stresses will be used in turbulence and sediment transport models of this area and relatively small changes in bottom stress can lead to large effects in transport. The S4DW data discussed addresses the comparison between model and data but there still remain questions as to which model for bottom friction is optimum. It is important to get the right amount of dissipation overall whereas the interaction modulation is a much smaller component and it is difficult to separate the effects of bottom friction from other shoaling effects.

7. Wave–current monitoring systems

Methods of remote sensing of waves include ground-based radar (HF and X-band), and satellite-based SAR and altimetry as described elsewhere in this volume. The advantage of remote sensing is the spatial coverage which may be obtained and potentially the simultaneous information on various parameters, e.g., waves, currents and bathymetry. Conversely, the measurements are not as direct as in situ measurements and may rely on complex inversion algorithms (e.g., Wyatt, 1997), based on certain assumptions about the initial form of the wave spectrum for example.

HF and X-band radar exploit the back-scattering of ground wave radio signals by sea-surface topography. HF radar can provide accurate surface current measurements over ranges of up to 70 km with spatial resolution of O (1 km) (Prandle, 1997b). Recent developments (Wyatt, 1997) enable directional wave spectra to be determined from these radars over a more limited range of up to 20 km. X-band radar (microwave or ship's radar) can be used to provide directional wave-length spectra at ranges of up to several kilometers. The displacement of the dispersion shell of the 3D wave-number-frequency spectrum enables currents to be determined (Young et al., 1985). In 'shallow' water (depth $< 1/2$ wavelength), the dispersion of long-crested swell waves also allows underlying bathymetry to be estimated (Bell, this volume).

Thus, direct monitoring of wave–current interactions is possible, together with synoptic monitoring of the prevailing, evolving bathymetry. X-band radar provides a basis for measuring both wave spectra and underlying current speed. Likewise, synthetic aperture radar (SAR) imagery can be interpreted in similar fashion (e.g., Shemer et al., 1993). Both techniques are better suited to observing wave directions and spectra of wave lengths than wave amplitude and both work better for longer period long-crested waves. SAR can be deployed from aircraft or satellite, the latter giving resolution of longer waves only.

Incorporation of wave influence on coastal tidal currents will require fine-scale resolution of waves, tides, bathymetry and sea bed conditions. Such resolution must be provided from shallow water versions of wave propagation models (e.g., WAM, SWAN [Booij et al., 1998; Ris et al., 1998]) with verification against comparable radar observations or against a series of in situ moorings which determine the progressive coastwards increase in these interaction effects.

Accurate fine-resolution tidal current models are now well-developed (e.g., Davies et al., 1997) and can be used to provide input to remove current modulation of wave recordings. However, noting the extent of the mutual wave–current interactions described above, the usefulness of incorporating a current meter coincident with any in situ wave measuring device is evident.

8. Summary

In (Prandle, 1997a), it was noted that waves are only likely to influence tidal currents (via bottom friction effects) in depths of less than 50 m. Significant influences can generally be anticipated in depths of less than 20 m at which point wave velocities are dispersive for waves with periods greater than 6 s. Thus, the relevant wave orbital velocity in these coastal regions of shallow water interaction will itself continuously adjust to the shallowing bathymetry.

Some effects which appear characteristic of wave–current interaction have been observed in the wave datasets collected during the SCAWVEX project. Reference has been made in particular to the in situ data collected at N1 and N2 (water depth 12.5 m and 18 m, respectively) at Holderness during two consecutive winters. The tidal modulation of various wave parameters (including wave height, period, steepness and direction) can be observed.

(i) The effect of waves on currents can be seen in an apparent decrease in tidal current amplitude with increasing wave height. This is attributed here to an increased bottom friction coefficient for the current flow due to the presence of waves. The observations agree qualitatively with the theory of Grant and Madsen (1979) and Christoffersen and Jonsson (1985) although further work on the quantification of these effects is required.

(ii) The effect of currents on waves is evident in the tidal modulation of significant wave height and especially in wave period. This can be quantified by means of Fourier analysis. The modulation of apparent (absolute) period must be attributable to the unsteady current.

(iii) The variation in steepness of the waves due to the Doppler shift of relative (intrinsic) frequency is shown to be correlated with the relative current with a phase lag of about 3 h.

(iv) The apparent frequency is misleading when trying to interpret the wave data. It is necessary to convert to intrinsic frequency which is a more physically meaningful parameter, related directly to the wavelength. To obtain this, it is essential to have simultaneous current information.

(v) The variation of high frequency wave direction seems consistent with current refraction of the waves. The maximum turning effect is seen when the currents and waves are at approximately 45°.

The monitoring of waves and currents simultaneously in shallow water is strongly recommended. Future real-time monitoring systems could include a remote sensing system such as HF radar and may also incorporate models and in situ ground-truth data.

Acknowledgements

The work described here was part of the EC MAST 2 SCAWVEX project. The Holderness data were collected for the Ministry of Agriculture, Fisheries and Food under its Flood Protection Commission.

References

Booij, N., Holthuijsen, L.H., Padilla-Hernandez, R., 1998. Numerical wave propagation on a curvi-linear grid. WAVES '97, pp. 286–294.

Burrows, R., Hedges, T.S., 1985. The influence of currents on ocean wave climates. Coastal Engineering 9, 247–260.

Christoffersen, J.B., Jonsson, I.G., 1985. Bed friction and dissipation in a combined current and wave motion. Ocean Engineering 12 (5), 387–423.

Davies, A.M., Flather, R.A., Kwong, S.C.M., 1997. A three-dimensional model of diurnal and semidiurnal tides on the European shelf. Journal of Geophysical Research C (Oceans) 102 (4), 8625–8656.

Grant, W.D., Madsen, O.S., 1979. Combined wave and current interaction with a rough bottom. Journal of Geophysical Research 84 (C4), 1797–1808.

Hasselmann, K., Barnett, T.P., Buows, E., Carlson, H., Cartwright, D.E., Enke, K., Ewing, J.A., Gienapp, H., Hasselmann, D.E., Kruseman, P., Meerburg, A., Müller, P., Olbers, D.J., Richter, K., Sell, W., Walden, H., 1973. Measurements of wind-wave growth and swell decay during the Joint North Sea Wave Project (JONSWAP). Deutsches Hydrographische Zeitschrift 8 (12), 95, Suppl. A.

Hedges, T.S., 1987. Combinations of waves and currents: an introduction. Proceedings of the Institute of Civil Engineers, Part 1 82, 567–585.

Hedges, T.S., Lee, B.W., 1992. The equivalent uniform current in wave–current computations. Coastal Engineering 16 (3), 301–311.

Hubbert, K.P., Wolf, J., 1991. Numerical investigation of depth and current refraction of waves. Journal of Geophysical Research 96 (C2), 2737–2748.

Janssen, P.A.E.M., 1989. Wave-induced stress and the drag of air-flow over sea waves. Journal of Physical Oceanography 19, 745–754.

Jonsson, I.G., 1990. Wave–current interactions. In: Le Mehauté, B., Hanes, D.M. (Eds.), 'The Sea'. Chap. 3, Vol. 9, Part A.

Komen, G.J., Cavaleri, L., Donelan, M., Hasselmann, K., Hasselmann, S., Janssen, P.A.E.M., 1994. Dynamics and modelling of ocean waves. Cambridge Univ. Press, 532 pp.

Luo, W., Flather, R.A., Monbaliu, J., 1997. An efficient computational scheme for the use of the third generation WAM-model in coastal regions. Submitted for publication in the Journal of Waterway, Port, Coastal and Ocean Engineering.

Madsen, O.S., 1995. Spectral wave–current boundary layer flows. ICCE 1994 Conference Proceedings, Chap. 29, pp. 384–398.

Phillips, O.M., 1977. The Dynamics of the Upper Ocean. Cambridge Univ. Press, 336 pp.

Prandle, D., 1982. The vertical structure of tidal currents. Geophysical and Astrophysical Fluid Dynamics 22, 29–49.

Prandle, D., 1997a. The influence of bed friction and vertical eddy viscosity on tidal propagation. Continental Shelf Research 17 (11), 1367–1374.

Prandle, D., 1997b. Tidal and wind-driven currents from OSCR. Oceanography 10 (2), 57–59.

Prandle, D., Wolf, J., 1978. The interaction of surge and tide in the North Sea and River Thames. Geophysical Journal of the Royal Astronomical Society 55, 203–216.

Ris, R.C., Holthuijsen, L.H., Booij, N., Andorka Gal, J.H., de Jong, J.C.M., 1998. The SWAN wave model verified along the southern North Sea coast, WAVES '97, pp. 49–63.

Shemer, L., Marom, M., Markman, D., 1993. Estimates of currents in the nearshore ocean region using interferometric synthetic aperture radar. Journal of Geophysical Research 98 (C4), 7001–7010.

Soulsby, R.L., Hamm, L., Klopman, G., Myrhaug, D., Simons, R.R., Thomas, G.P., 1993. Wave–current interaction within and outside the bottom boundary layer. Coastal Engineering 21, 41–69.

Tolman, H.L., 1990. The influence of unsteady depths and currents of tides on wind-wave propagation in shelf seas. Journal of Physical Oceanography 20, 1166–1174.

Tolman, H.L., 1991a. A third-generation model for wind waves on slowly varying, unsteady, and inhomogeneous depths and currents. Journal of Physical Oceanography 21, 782–797.

Tolman, H.L., 1991b. Effects of tides and storm surges on North Sea wind waves. Journal of Physical Oceanography 21, 766–781.

Tolman, H.L., 1992. An evaluation of expressions for wave energy dissipation due to bottom friction in the presence of currents. Coastal Engineering 16, 165–179.

Wolf, J., 1997. The analysis of bottom pressure and current data for waves. Proceedings of IEE Conference on Electronic Engineering in Oceanography, Southampton, June 1997.

Wolf, J., 1998. The analysis of near-bed turbulent currents for combined wave–current flows, this volume.

Wolf, J., Hubbert, K.P., Flather, R.A., 1988. A feasibility study for the development of a joint surge and wave model. Proudman Oceanographic Laboratory Report, No. 1, 109 pp.

Wolf, J., Hargreaves, J.C., 1998. Modelling waves at holderness. Proudman Oceanographic Laboratory Internal Document, No. 130, 13 pp.

Wyatt, L.R., 1997. The ocean wave directional spectrum. Oceanography 10 (2), 85–89.

Young, I.R., Rosenthal, W., Ziemer, F., 1985. A three-dimensional analysis of marine radar images for the determination of ocean wave directionality and surface currents. Journal of Geophysical Research 90 (C1), 1049–1059.